

We are IntechOpen, the world's leading publisher of Open Access books Built by scientists, for scientists

6,100

Open access books available

149,000

International authors and editors

185M

Downloads

Our authors are among the

154

Countries delivered to

TOP 1%

most cited scientists

12.2%

Contributors from top 500 universities



WEB OF SCIENCE™

Selection of our books indexed in the Book Citation Index
in Web of Science™ Core Collection (BKCI)

Interested in publishing with us?
Contact book.department@intechopen.com

Numbers displayed above are based on latest data collected.
For more information visit www.intechopen.com



Chapter

The Present Situation and Development for Spaceborne Synthetic Aperture Radar Antenna Arrays

*Hua Li, Zhenning Li, Kaiyu Liu, Mingshan Ren
and Yunkai Deng*

Abstract

Synthetic aperture radar (SAR) based on satellites and or space vehicles as motion platform has the capability to work under all weather conditions, day and nights, and has become an indispensable mean for earth observation. At present, the large-scale phased array antenna, such as the active microstrip-phased array antenna of SIR-C imaging radar and the waveguide slot-phased array antenna of Radarsat-1 imaging radar, is one of the core components of spaceborne SAR and determines the system performance to a large extent. Although the traditional antenna array scheme has been widely used in existing spaceborne SAR systems due to strong beam control ability, sufficient failure redundancy backup, mature design method and so on, it still has drawbacks, for example, large volume, high weight and manufacturing cost, and low energy utilization rate, which restrict the further improvement of performance and are burdens on the research of next-generation high-performance spaceborne SAR system. With the development of electric and electronic techniques, forthcoming SAR array-phased array antennas will make breakthroughs in antenna architectures, concepts, technologies and modes, for instance, periodic reflector array antennas and metamaterial array antennas. This chapter focuses on the present and forthcoming development of spaceborne SAR antenna arrays.

Keywords: spaceborne synthetic aperture radar, antenna arrays, beamforming, metamaterials, high-resolution wide-swath

1. Introduction

In 2018, an English named Ian Wilson claimed that he had found the MH370 passenger plane which had been missing for four and a half years on Google maps and it was located in a dense forest in Cambodia. The news caused a sensation on the global Internet. Changguang Satellite Technology Co., Ltd. immediately maneuvered

all 10 satellites to observe this area one after another. Unfortunately, the first photos were disappointing. The authenticity of the rumor could not be confirmed because the suspected crash site of MH370 was covered by clouds. This dramatic event reminded people of synthetic aperture radar (SAR), because it can make up for the shortcomings of optical earth observation by the capability to pass through all kinds of obstacles such as clouds, rain, snow, fog, sand, dust, and so on and to work under all weather conditions, day and nights [1–3].

Spaceborne SAR equipped on low/medium orbit satellites or other orbital platforms such as space shuttle, the upper stage of the launch vehicle, and so on is a kind of advanced earth observing and imaging system [4–6]. It has played an irreplaceable role in the fields of global military reconnaissance, environmental remote sensing, natural disaster monitoring, and planetary exploration and gradually become a research hotspot in the field of earth observation since the United States launched the first SAR satellite SeaSat in 1978 [7, 8]. Many countries have successively carried out spaceborne SAR technology research and formulated corresponding development plans of the SAR satellite system. In the 21st century, many countries have successively deployed their own spaceborne SAR satellite systems and realized the upgrading of SAR satellites. For example, European Space Agency (ESA) launched Sentinel-1 to replace ENVISAT [9]. In recent 10 years, spaceborne SAR has made great progress in hardware structure, imaging theory, system performance, and application fields. It is worth noting that only the TecSAR system adopts the reflector antenna and the rest are phased array antenna [5]. In fact, an array antenna is the main configuration scheme for most modern high-performance spaceborne SAR, because it is preferred to obtain better performance within the limited mission budget [10, 11]. This chapter focuses on the development trend of array antenna technology of spaceborne SAR and discusses the research status in the future from the aspects of system composition, antenna performance, planar phased array antenna, paraboloid array antenna, and metasurface array antenna.

2. Spaceborne SAR antenna subsystem technical features

Spaceborne SAR system usually consists of operation loads and function loads. The former mainly serves the spaceborne platform operation, such as the attitude and orbit control subsystem, telemetry control subsystem, environmental control subsystem, power subsystem, and so on. The function loads directly related to SAR imaging processing are usually composed of the following subsystems:

- SAR antenna subsystem

It can radiate the radar pulse signal generated by the front-end subsystem and receive the corresponding radar echo signal. The antenna needs to be able to meet the strict requirements of beam scanning and shaping for spaceborne SAR.

- Radio-frequency signal generating and processing subsystem

According to the task requirements, it generates the modulated pulse signal transmitted by the SAR antenna and down converts as well as samplings the received original radar echo signal. After analog-to-digital conversion, the original imaging

data are obtained, which is handed over to the rear terminal system for imaging processing.

- Signal processing and imaging subsystem

It completes the imaging and image information compression processing of the original data in a high-performance data processor.

- Data handling and transmission subsystem

It stores the image information as well as other relevant data and transmits them to the ground receiving station.

Figure 1 shows the photo of Canada's Radarsat-2 satellite and deployable 12 m × 3 m lightweight SAR membrane antenna. The long strip structure covered with gold foil below is C-band SAR Antenna.

The SAR antenna subsystem which occupies a considerable amount of mass as well as volume and consumes the most power during operation is the most difficult, time-consuming, and costly part, due to the stringent requirements on antenna performance. In general, spaceborne SAR mainly has the following technical features:

- Wide observation strip and large observation area

The commonly observed swath width can reach 40 km or more and the length of continuous imaging area can reach thousands of kilometers. Through antenna beam scanning and satellite platform maneuver, the width of the observable area can reach 500–600 km, including more than 10 common observation strips [7].

- Far slant range and high signal transmission path loss

For example, for a spaceborne SAR system with a center frequency of 9.6 GHz, an orbit height of 600 km, and an antenna look angle of 25°–45°, the slant range

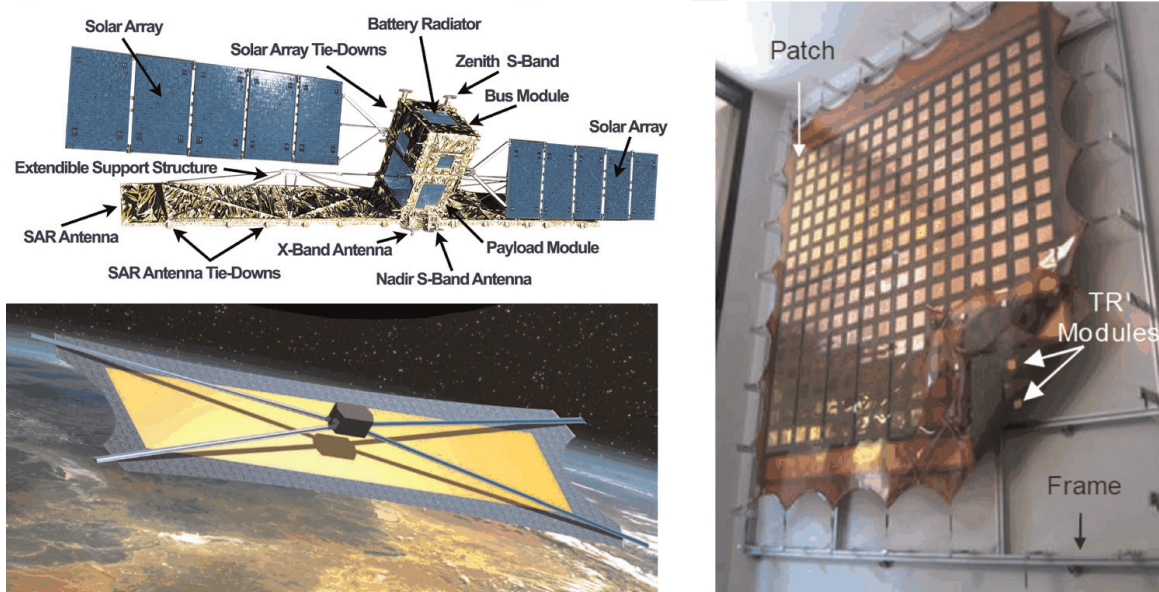


Figure 1.
Canada's Radarsat-2 satellite and deployable SAR Membrane Antenna.

between the antenna to the observation area is 670–890 km and the two-way path loss is 168–170 dB.

- Long revisit cycle period

The satellite platform runs along the preplanned orbit and can only observe the same area once in a revisit cycle. Even if the orbit planning is reasonable and the antenna beam has good adjustment ability, the typical revisit cycle of spaceborne SAR still ranges from 2 to 3 days to more than 10 days [7, 8]. If forced orbit change is required to shorten the revisit period, additional satellite fuel will be consumed and the system life and mission duration will be shortened.

- Serious ambiguity signal interference

Spaceborne SAR system faces inherent ambiguity signal problems, including range ambiguity and azimuth ambiguity. The intensity and distribution of the ambiguous signal are affected by the width of the imaging area, pulse repeat frequency, pulse width, pulse bandwidth, look angle, backscattering coefficient, and other parameters [12]. Most of the above parameters restrict each other and are difficult to control independently. In order to reduce the ambiguity signal ratio to meet the system index requirements, it is necessary to decrease the SAR antenna pattern sidelobe to the source direction of the ambiguity signal.

- Various working modes

Currently, spaceborne SAR systems in operation or under development can generally work in Stripmap mode, ScanSAR mode, Spotlight mode, etc. Each mode has different requirements for antenna beam characteristics [13]. **Figure 2** displays the corresponding beam diagrams of five spaceborne SAR operating modes given from left to right, including huge region ScanSAR mode, wide region ScanSAR, himage Stripmap mode, polarimetric Stripmap mode, and spotlight mode. Generally

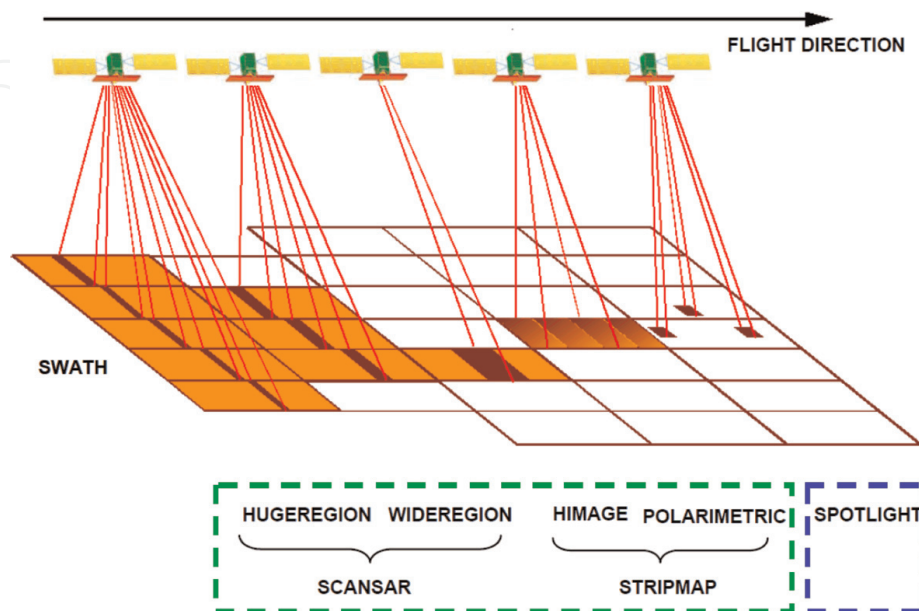


Figure 2.
Various working modes for spaceborne SAR.

speaking, according to different task requirements, the scanning beam ranges from several degrees to tens of degrees in the range direction while the azimuth beam scans within several degrees.

- Wide frequency band

In order to meet different mission requirements, the commonly used spaceborne SAR operating frequency band spans from P-band to X-band. Electromagnetic waves with different frequency bands have different penetrating abilities. Generally speaking, the higher the frequency, the wider the bandwidth and the higher the resolution, but the weaker the penetration ability to vegetation and other covers. Ku, K, and Ka band spaceborne SAR satellites with higher resolution belong to the next generation system under research have not been widely used at present.

- Full polarimetric signal processing

In addition, with the development of SAR target polarimetric information processing technology, more and more spaceborne SAR systems have the ability of full polarimetric signal processing.

According to the above technical features of the spaceborne SAR system, a series of strict performance requirements of array antenna is determined as follows:

- Narrow beam and high gain

In order to compensate for the extremely high path loss, the spaceborne SAR antenna needs to have a very high gain. Taking the X-band TerraSAR-X system launched in 2007 as an example [8], its SAR antenna in **Figure 3** size is 4.8×0.75 m and the antenna normal gain exceeds 46 dBi. At the same time, in order to suppress the ambiguous signal and improve the imaging quality, the spaceborne SAR antenna has strict restrictions on the maximum width of the main beam for range and azimuth. In addition, COSMO-SkyMed's, which was launched in 2007 and works in X-band [14], antenna size is 5.7×1.4 m. The average width of the range beam is 1.5° and the average width of the azimuth beam is only 0.3° .

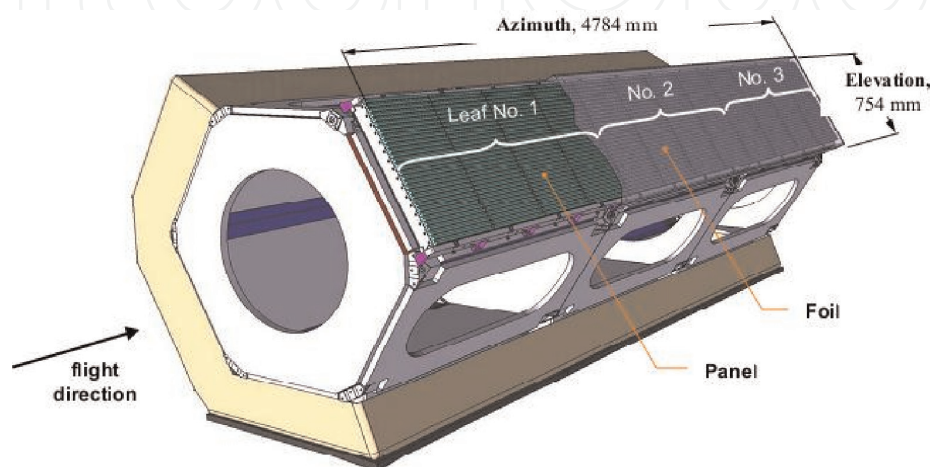


Figure 3.
Diagram of antenna structure for TerraSAR-X.

- Beamforming and sidelobe suppression

The sidelobe level in the source direction of the ambiguity signal needs to be especially suppressed to ensure that the ambiguity signal ratio meets the system index requirements. Compared with TX pattern, which takes the maximization of effective isotropic radiation power (EIRP) as the design guide and does not particularly consider sidelobe suppression, the RX pattern in **Figure 4** has to carry out a wide range of sidelobe suppression in the main range direction of ambiguity signal source. At the same time, in order to ensure that the echo signal level in the imaging area does not exceed a certain range to ensure the imaging quality, the main beam lobe needs to be shaped and adjusted, which makes the amplitude of the pattern point to the far end for the observation area appropriately higher than that pointing to the near end, so as to compensate for echo signal attenuation caused by larger path loss and smaller ground friction angle [15].

- High EIRP of TX antenna and high G/T value of RX antenna

In order to ensure that the spaceborne SAR system can successfully complete the imaging mission, the actually received signal power and signal-to-noise ratio of the data acquisition device need to meet the minimum requirements, which involves two factors that, first, the EIRP of the TX antenna should be high enough, that is, in addition to the high gain, the actual transmitting power of the antenna should also reach a high level. On the other hand, in order to achieve a sufficient signal-to-noise ratio of the received signal, the RX antenna is required to have a sufficiently high G/T value.

- Full polarimetric mode

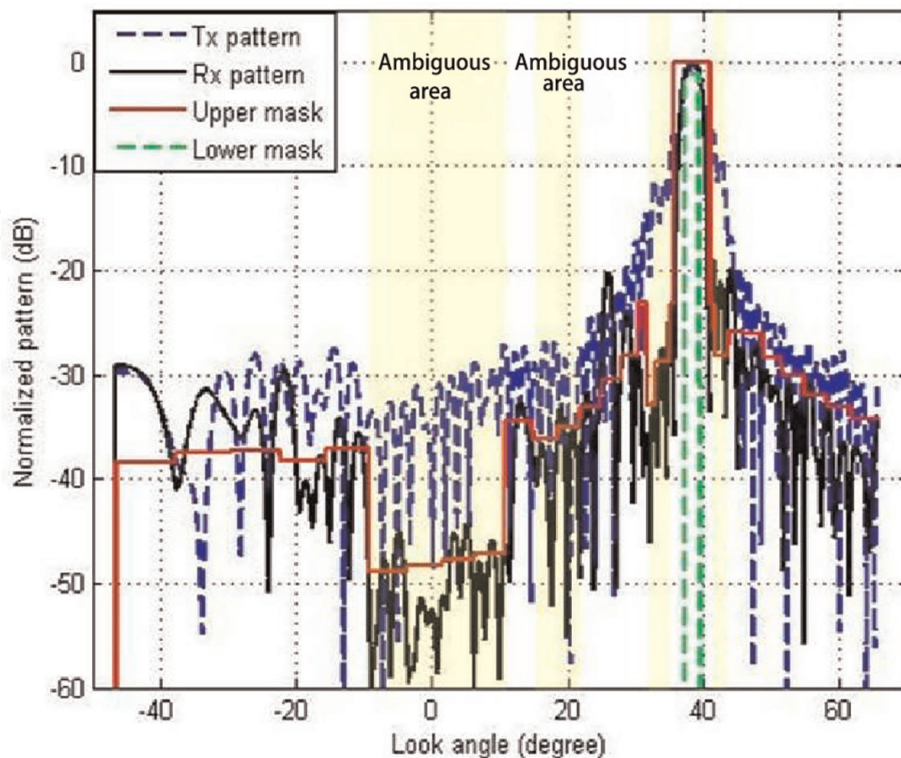


Figure 4.
Range beam pattern of typical SAR Antenna.

Early spaceborne SAR systems, such as SeaSat in 1978 and SIR-C in 1981, used a single polarimetric antenna. In recent years, as more and more spaceborne SAR systems have the ability of full polarimetric signal processing, there is an urgent need for the full polarimetric performance of SAR Antenna. At present, there are two main types of spaceborne SAR antenna: microstrip patch array antenna and waveguide slot array antenna. The former, represented by COSMO-SkyMed in **Figure 5** [7] and Radarsat-2 [6], is usually a double-layer microstrip patch array based on lightweight dielectric materials [16, 17]. It has the advantages of light structure weight, dual-polarization, flexible arrangement of elements and subarrays, etc., but it has a slightly larger loss compared with the other scheme. The latter is represented by TerraSAR-X [18] and sentinel-1 in **Figure 6** [19, 20]. The ridged waveguide wide-edge slot antenna [21] and the reduced waveguide narrow-edge slot antenna made of carbon fiber reinforced plastic [22, 23] are alternately arranged to form a dual polarimetric array antenna, which has low loss and high radiation efficiency, but it is slightly heavy, difficult to design as well as process and difficult to adjust the position of array elements and subarrays.

- Limited range scanning angle and small azimuth scanning angle

The orbit altitude of spaceborne SAR platform is usually between 500 and 800 km. Due to the limitations of earth curvature and range resolution, the antenna beam in the range direction, that is, the direction on the elevation plane, is usually within the range of 15° – 50° starting from the connecting line between the satellite and the nadir on the earth's surface, with a span of 35° . Limited by the Doppler bandwidth of the processed echo signal, the beam coverage and scanning range in the azimuth, that is, horizontal plane, are usually within $\pm 2^{\circ}$ [5, 7, 17]. Compared with the phased array

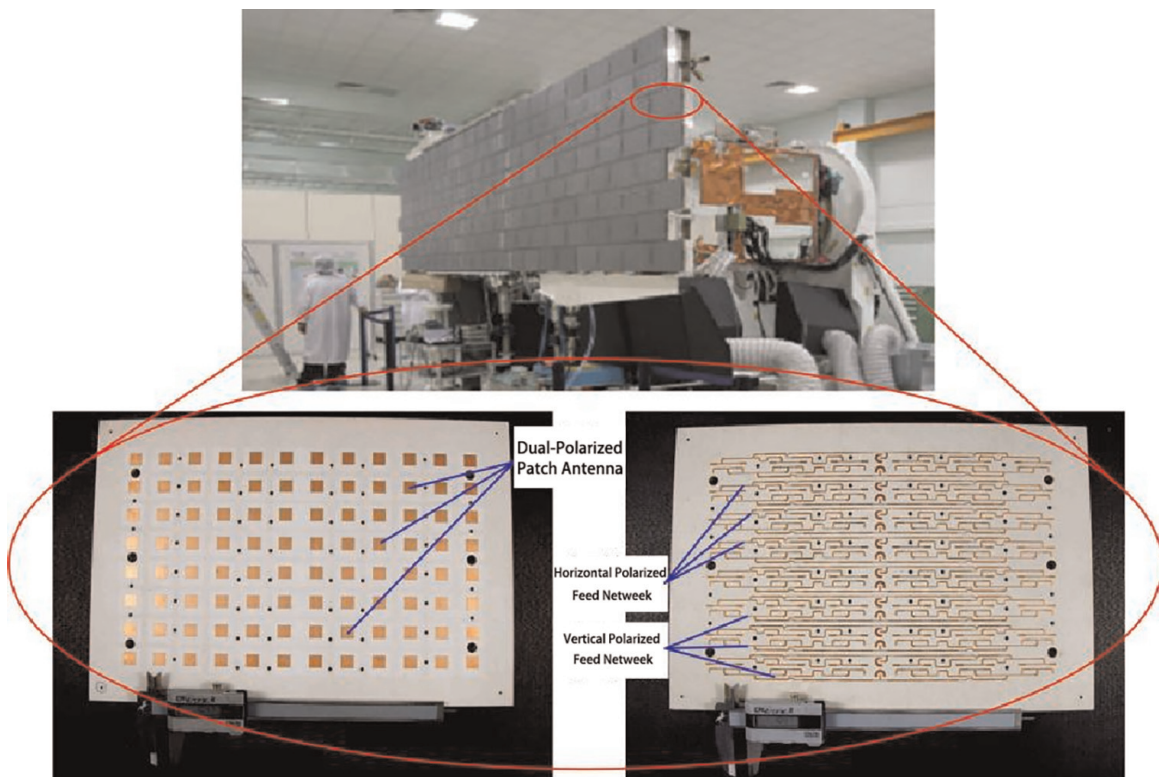


Figure 5.
Photo of microstrip patch array SAR antenna of COSMO-SkyMed.

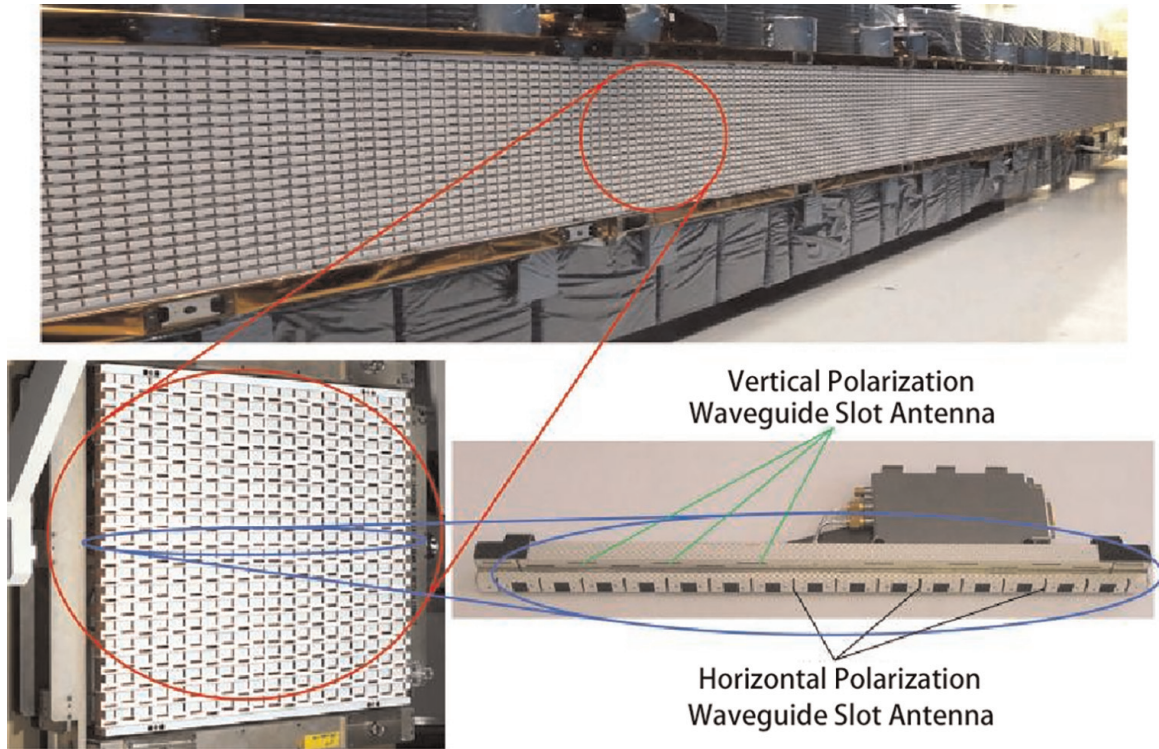


Figure 6.
Photo of waveguide slot array SAR antenna of Sentinel-1.

antenna of other applications, such as warning/fire control radar, the scanning range of spaceborne SAR antenna is limited in range and very small in the azimuth.

3. Technical features and development of spaceborne SAR planar phased array antenna

Planar phased array antenna has been widely used in spaceborne SAR systems and its superior performance has been fully demonstrated and verified. **Table 1** summarizes the features and technical parameters of some spaceborne SAR antennas using planar phased array antennas.

Planar phased array antenna uses a medium-scale line array as the basic unit to form a full-scale area array. Since the scanning angle of the azimuth beam is very small, according to the basic principle of the phased array antenna, the size of the array element in this direction or the phase center spacing of the adjacent array elements can be expanded to achieve the purpose of reducing the number of control channels without reducing the number of control channels. Grating lobes appear when the beam is scanned. The scanning angle of the distance beam is relatively large, and it is necessary to ensure that the phase center spacing of adjacent units is less than 0.8 times the wavelength of the center frequency to ensure that the sidelobe performance does not deteriorate excessively during beam scanning. Therefore, the current mainstream spaceborne SAR phased array antennas usually use 10–20 minimum radiating elements (microstrip patches or waveguide slots) to form a linear array, and the excitation of each element inside the linear array cannot be controlled independently. After that, the linear array is used as the basic unit of the full-size antenna to control the amplitude and phase of each linear array. Generally speaking, there are 12–

Working waveband	Name	Center frequency (GHz)	Pulse bandwidth (MHz)	Relative bandwidth (%)	Range of view angle (°)	Antenna element type	Antenna size (m ²)	Launch time
P	Seasat	1.275	19	1.5	20–26	microstrip patch	10.7 × 2.2	1978
	SIR-A	1.275	6	0.47	47–53	microstrip patch	9.4 × 2.16	1981
	JERS-1	1.275	15	1.2	32–38	microstrip patch	11.9 × 2.2	1992
	PALSAR	1.27	28	2.2	9.9–50.8	microstrip patch	—	2006
S	NovaSAR-S	3.2	200	6.25	16–34	microstrip patch	3 × 1	2013
C	ERS-1/2	5.3	15.55	3	20.1–25.9	waveguide slot	11 × 1.3	1991/1995
	RADARSAT-1	5.3	30	0.57	20–58	microstrip patch	15 × 1.5	1995
	RADARSAT-2	5.405	100	1.85	20–50	microstrip patch	15 × 1.37	2007
	ENVISAT	5.331	124	2.32	15–45	microstrip patch	10 × 1.3	2002
	SENTINEL-1	5.405	100	1.85	20–45	waveguide slot	12.3 × 0.9	2014
X	COSMO-SkyMed	9.6	400	4.17	19–49	microstrip patch	5.7 × 1.4	2007
	TerraSAR-X	9.65	300	3.1	25–55	waveguide slot	4.8 × 0.7	2007
	Paz	9.65	300	3.1	25–55	waveguide slot	4.8 × 0.7	2017

Table 1.
 The features and technical parameters of spaceborne SAR antennas.

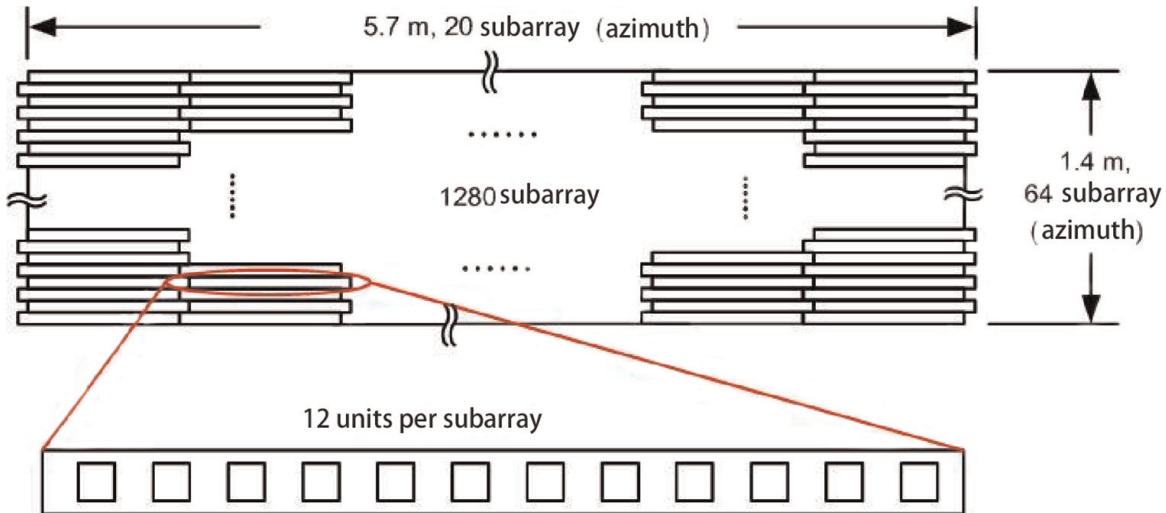


Figure 7.
Conceptual schematic diagram of COSMO-Skymed phased array antenna.

20 line arrays along the azimuth direction, and 30–64 line arrays along the distance direction. The entire array can have 300 to more than 1000 line arrays and corresponding amplitude and phase control channels, and more than 10,000 actual minimum radiation unit (microstrip patch or waveguide slot). **Figure 7** shows a conceptual schematic diagram of the COSMO-Skymed phased array antenna structure. The antenna consists of 64 (elevation plane) \times 20 (azimuth plane) a total of 1280 line arrays, each line array contains 12 basic radiating elements. All line arrays are arranged in the horizontal (azimuth plane) direction. Note that in order to improve the grating lobe performance, a staggered arrangement is used between adjacent linear arrays on the pitch plane, but in principle, it is still a planar linear array.

In addition, its relative bandwidth is not large. At present, the relative bandwidth of the transmitted pulses of spaceborne SAR systems using phased array antennas usually does not exceed 5%. For example, COSMO-Skymed has a working center frequency of 9.6 GHz, a maximum bandwidth of 400 MHz and a relative bandwidth of 4.2%. Sentinel-1 has a working center frequency of 5.405 GHz, a maximum bandwidth of 100 MHz and a relative bandwidth of 1.85% [4, 19]. In fact, this is also an inevitable limitation brought by the use of medium-scale linear arrays as the minimum amplitude and phase control unit system. For example, the bandwidth of a waveguide slot antenna with more than 15 slots is difficult to exceed 6% [24]. The Nova-SAR with a smaller antenna size (3×6 linear arrays, each with 24 patch elements) has the widest working bandwidth among spaceborne SAR systems equipped with microstrip patch phased array antennas and its working center frequency is 3.2 GHz. The maximum bandwidth is 200 MHz and the relative bandwidth is 6.25% [3].

However, the traditional spaceborne SAR periodic array phased array antenna still has the following shortcomings:

- Expensive

The total price of a large number of high-performance RF active devices is so considerable that some spaceborne SAR users with urgent needs and limited budgets can only use other antenna solutions [5].

- Excessive total system weight and widely distributed mass

This aspect occupies a large proportion of the launch payload, but also makes the SAR satellites have a large moment of inertia and a high fuel consumption rate for maneuvering and attitude control during in-orbit operation [25–27].

- High Power consumption

When working at full power, the phased array antenna will consume most of the power supply of the satellite platform, and the peak power consumption far exceeds the power provided by the solar panels on the satellite. For this reason, SAR satellites are usually equipped with large-capacity batteries. The issue of power consumption has become one of the main factors limiting the working time of continuous imaging of spaceborne SAR. Taking the COSMO-Skymed system, which began to operate in orbit in 2007, as an example, the peak power required for SAR imaging observation in spotlight mode is 17.3 kW, and most of the energy is consumed by the phased array antenna (especially the transmitter); while the solar panels onboard the satellite can only provide a maximum of 4.5 kW (at the initial stage of the mission) to 3.5 kW (at the end of the mission). To make up for this gap, a lithium-ion battery with a capacity of 336 Ah is onboard the satellite. The battery weighs 136 kg, and the mass of the entire satellite at launch is only about 1700 kg (including fuel and propellant). Even with this power supply configuration, the COSMO-Skymed only lasts about 10 s of continuous imaging when operating in the most power-hungry spotlight mode, and only about 10 s when operating in the lower-power stripe mode. Minutes limit the information acquisition capability of spaceborne SAR to a large extent. One of the important reasons for this problem is that the transmit-receive power transition efficiency (TRPE) of the current mainstream spaceborne SAR periodic array phased array antenna is relatively low.

- Redundant system performance

As far as the general spaceborne SAR system needs to scan and shape the antenna beam, the periodic array phased array antenna is actually in a state of excess performance. Specifically, phased array antennas that achieve the smallest antenna aperture area of spaceborne SAR are of considerable size, usually containing more than 300, or even more than 1000 independent transceiver control channels. For a phased array antenna of this size, even if up to 10% of the transceiver units fail, the excitation of the remaining units can still be adjusted to roughly maintain the main radiation performance indicators of the antenna, such as beam deflection angle, main lobe width and the sidelobe level in the ambiguous area, which is equivalent to a certain amount of redundancy in the antenna performance. In the traditional concept of spaceborne SAR engineering practice, it is generally believed that the performance of some antenna unit components will gradually degrade or fail during the operation of the mission. At this time, it is necessary to release the redundant performance of the array to ensure that the SAR antenna function can still be properly used at the end of the mission cycle [28, 29]. Function properly. However, in recent years, with the development of advanced solid-state active RF circuit technologies such as Monolithic Microwave Integrated Circuit (MMIC), Low-Temperature Co-fired Ceramics (LTCC), and spaceborne SAR systems. With the improvement of orbital operation management experience, the reliability of phased array antenna units and radio frequency components used in spaceborne SAR is increasing day by day. The number

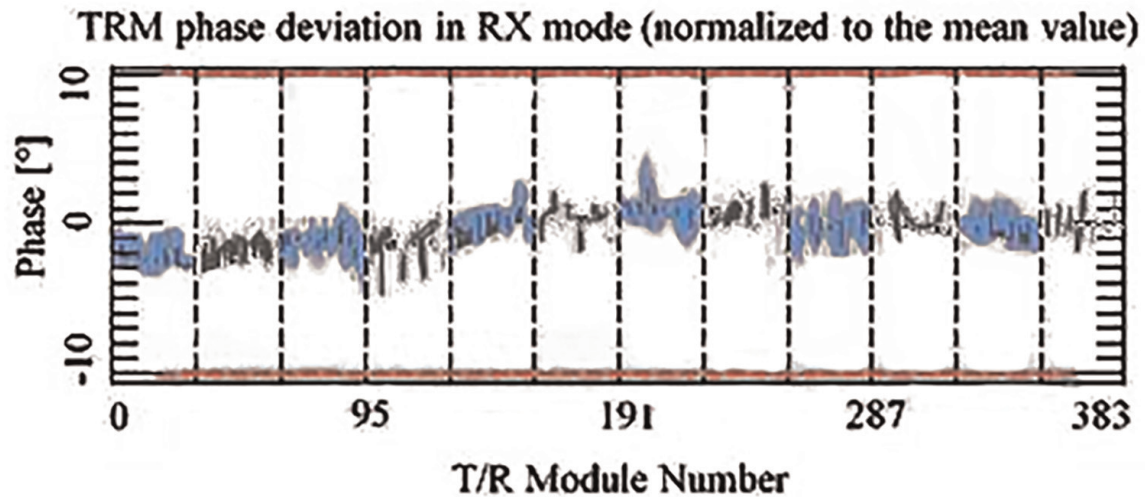


Figure 8.
Phase error test results of T/R components for TerraSAR-X (2016).

of failed units during the full mission cycle is often lower than expected during mission planning [30–33]. For example, the CosmoSky-Med (No. 1 Star) and TerraSAR-X systems [8], they were launched by ESA in 2007 and 2008 and then started operating, respectively. The original mission periods of the two satellites are only until 2012 [34, 35]. However, as of the end of 2016, it is still operating reliably in orbit, and the phased array SAR antenna carried is still in good condition. **Figure 8** shows the phase error test results of all 384 T/R components of TerraSAR-X in the eighth year (2016) in orbit. The phase errors of all channels are far less than the tolerance range of 10° (significant difference). Significant difference. It can be seen that the scale of the traditional spaceborne SAR phased array antenna has a certain compressible space under the condition of maintaining the system performance generally unchanged.

The deficiencies of large phased array antennas in the above four aspects have restricted the development and application of spaceborne SAR systems to a certain extent. Studies have shown that the above problems are expected to be improved when applying Uniform Amplitude/Equal Amplitude or Quantized Amplitude aperiodic array phased array antennas in spaceborne SAR systems [36–39]. The spacing between the elements of an Aperiodic Phased Array Antenna is usually not uniform [36, 38, 40, 41]. This is the most significant difference from the periodic array phased array. The number of aperiodic and periodic array elements of the same aperture is not necessarily the same. Generally speaking, the number of practical aperiodic array elements is less than or equal to that of the periodic array of the same aperture. When the number of aperiodic array elements is smaller than that of periodic arrays with the same aperture, it can also be called a thinned array or a sparse array. For sparse arrays, the element spacing is an integer multiple of a certain greatest common divisor; while for sparse arrays, the spacings of array elements are randomly distributed and have no greatest common divisor.

A series of studies have discussed the advantages of aperiodic array phased array antennas in reducing the number of active devices and improving energy utilization efficiency when applied to spaceborne SAR [36, 39, 42, 43] and synchronous satellite communication systems [37, 38, 44–52]. For these two types of applications, there are three things in common: (1) high-gain beams; (2) strict sidelobe control; and (3) beam scanning requirements over a relatively small angular range. In order to achieve

high-gain beams, the array antenna must have a larger aperture and a larger number of elements; strict sidelobe control means that the excitation amplitude of the antenna array must be significantly tapered; the beam scanning requirement of a smaller angle makes the restrictions on the maximum spacing of the antenna elements in the medium are looser. The above three characteristics make it possible to design aperiodic array antennas excited by equal amplitude [36] or quantized amplitude [38, 53] on the basis of tapered amplitude excitation periodic array antennas. Such aperiodic array antennas naturally have the advantages of reducing the number of active devices and improving energy utilization efficiency.

A widely studied and applied aperiodic array antenna design is the density tapering (Density Tapering) constant amplitude excitation aperiodic array antenna [39, 44, 54, 55]. Compared with the Amplitude Tapering periodic array antenna used as a design reference, a well-designed density-tapered equal-amplitude excited aperiodic array antenna has roughly equivalent gain and sidelobe performance, and can be used as an active transmit antenna. All high-power amplifiers are made to work at the saturation operating point of the highest efficiency so that the DC-RF Power Transition Efficiency (DC-RF Power Transition Efficiency) is higher than that of the traditional periodic array antenna whose excitation amplitude is tapered. **Figure 9** presents the results of a typical constant-amplitude excitation aperiodic array design [39]. Among them, the upper left is the comparison of the aperiodic array element position, excitation amplitude, and the reference excitation amplitude used as a reference to taper the periodic array; the upper right is the pattern of the aperiodic and periodic array antennas, especially the sidelobe performance comparison, it can be seen that

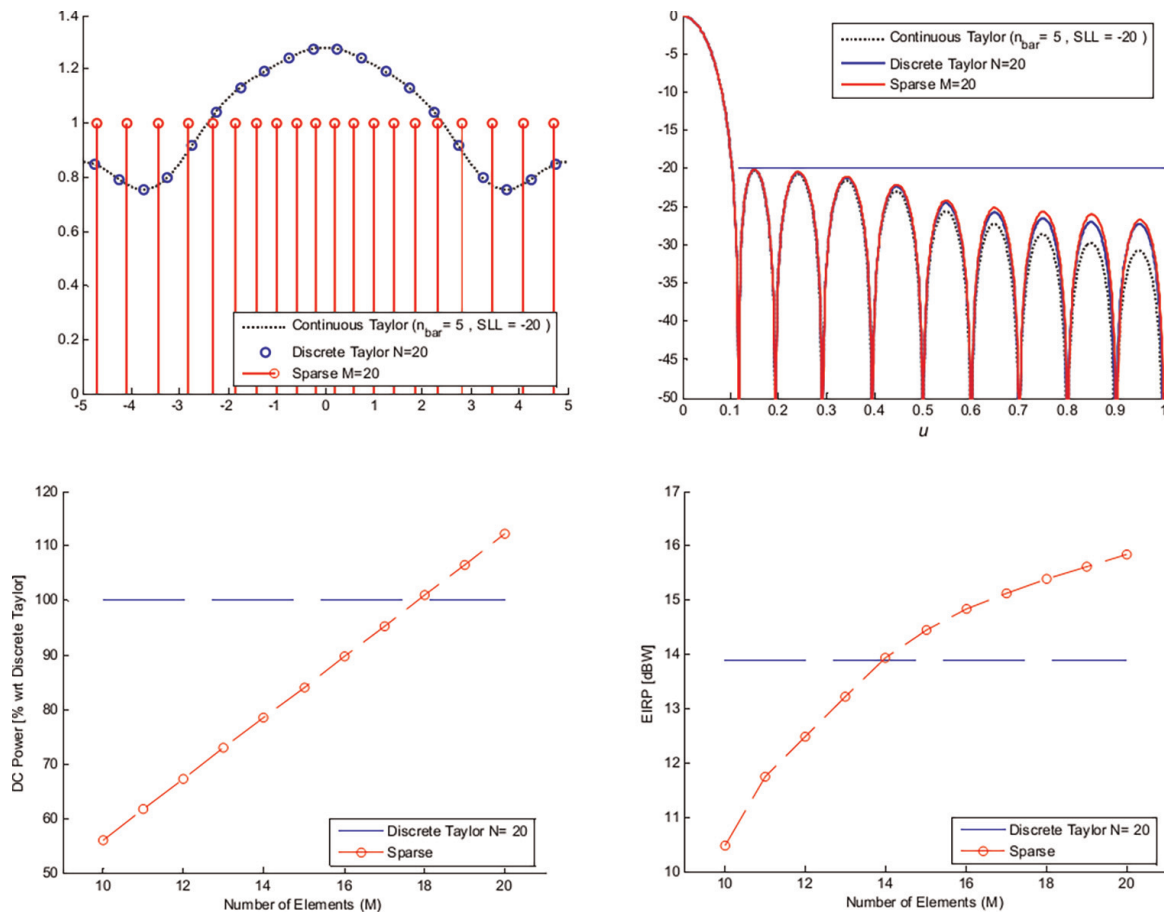


Figure 9. Example of density tapered aperiodic array antenna design results.

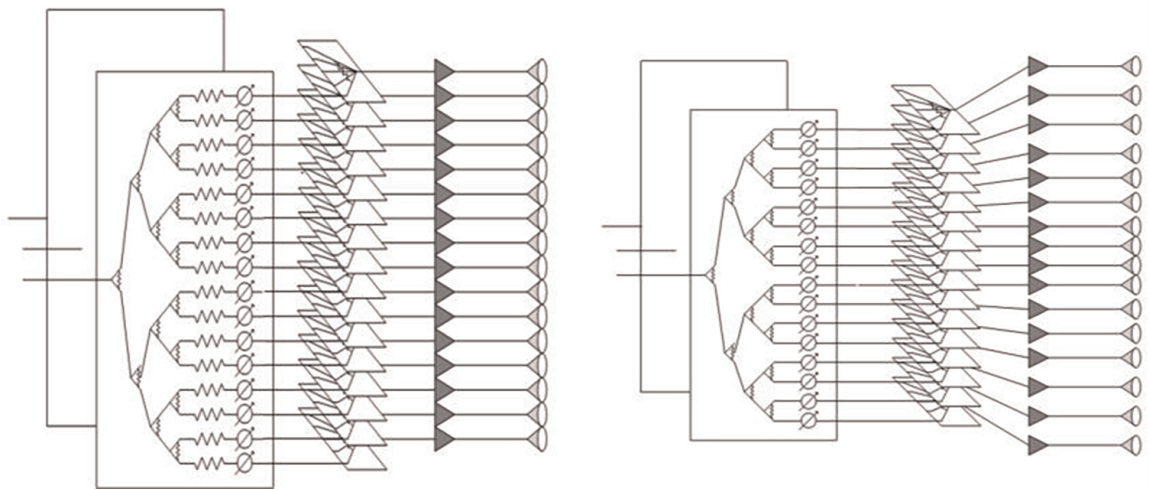


Figure 10.
Diagram of amplitude taper periodic array phased array and equal-amplitude aperiodic array phased array structure.

the two are basically equivalent; the lower left is the variation of the DC power consumption of the aperiodic array with the number of elements, and compared with the case of the 20-element periodic array, the lower right is the variation of the Equivalent Isotropic Radiation Power (EIRP) of the aperiodic array with the number of elements and is compared with the case of the 20-element periodic array. Compared with the 20-element periodic array, it can be seen that when the number of elements is between 14 and 18, the aperiodic array consumes less DC power than the 20-element periodic array and obtains a higher EIRP.

Compared with periodic array antennas, aperiodic array antennas have very different characteristics. As shown in the right of **Figure 10** [39], firstly, the analysis of the array characteristics can no longer be simplified to the processing of one element in the periodic boundary; secondly, the characteristics of each element in the aperiodic array are quite different; finally, the processing and Test work is also much more difficult and complex than periodic arrays. Despite the above difficulties, the research on aperiodic array antennas has still received extensive attention. In addition to the aforementioned advantages of reducing the number of radiation units or control units and improving the DC-RF conversion efficiency, the aperiodic array actually increases the degree of freedom in the design of the array antenna, so it is expected to obtain a more ideal array design result. Characteristics are also one of the reasons why it is studied.

In recent years, a group of European research institutions funded by ESA has carried out research on spaceborne aperiodic phased array antenna experimental systems mainly serving satellite communication systems. In 2010, a team of researchers from Naples University, Università di Cassino and Space Engineering S.P. A. reported the results of their preliminary development of an experimental system for satellite communications aperiodic array antennas. The designed aperiodic array antenna is composed of various aperture units, as shown in the left in **Figure 11**. The test results prove that the antenna design has high aperture efficiency and global beam coverage. The same group of researchers also completed the design of a multi-beam aperiodic dielectric lens antenna based on a similar theoretical design, as shown on the right in **Figure 11**. The experimental test results show that the performance of the designed aperiodic array antenna is basically the same as that of the periodic array antenna used for comparison, and the number of control devices is significantly reduced [37].

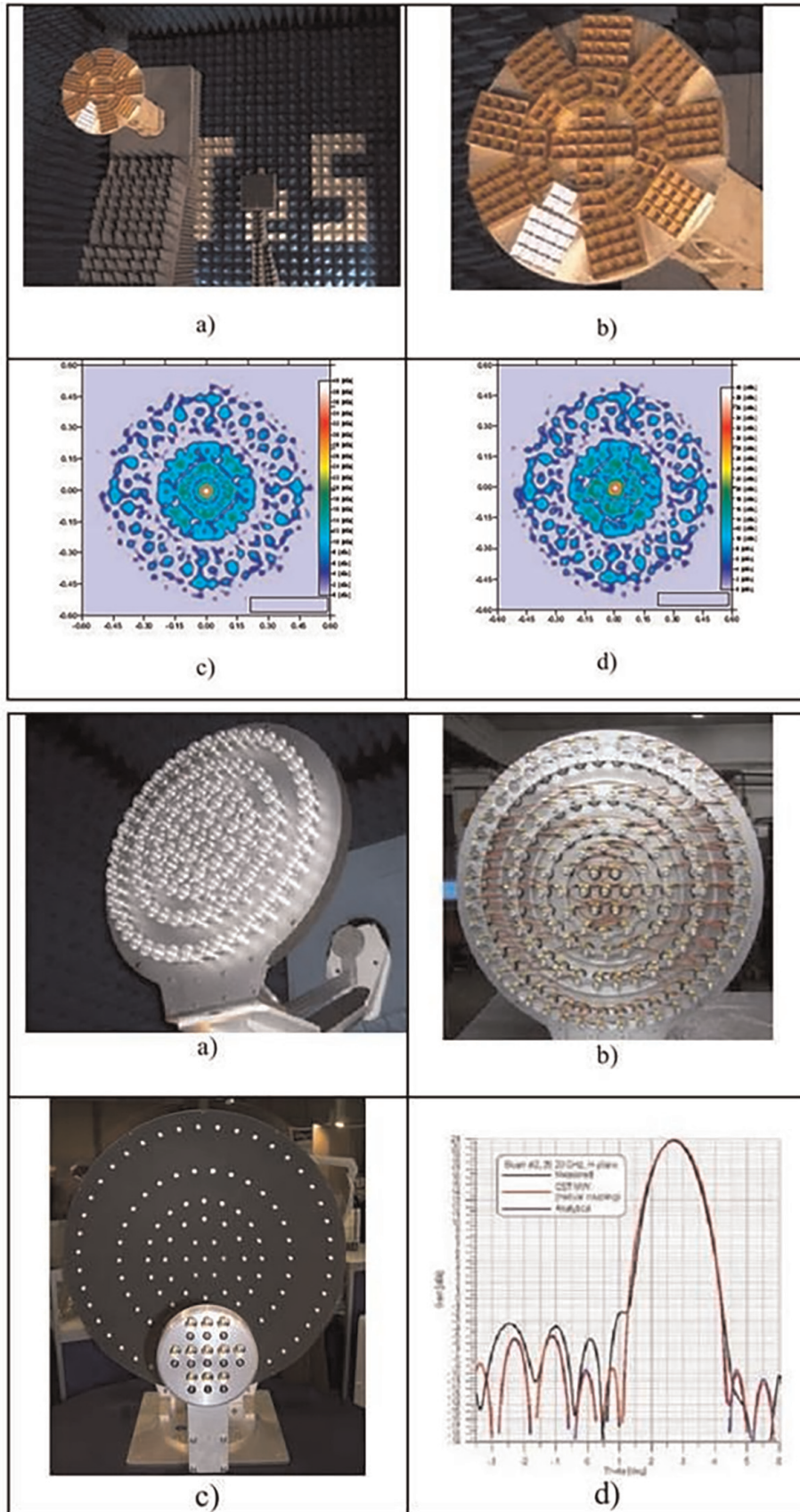


Figure 11. ESA satellite communication aperiodic array antenna experimental system hybrid unit direct radiation array and test results (left), aperiodic reflection array and test results (right).

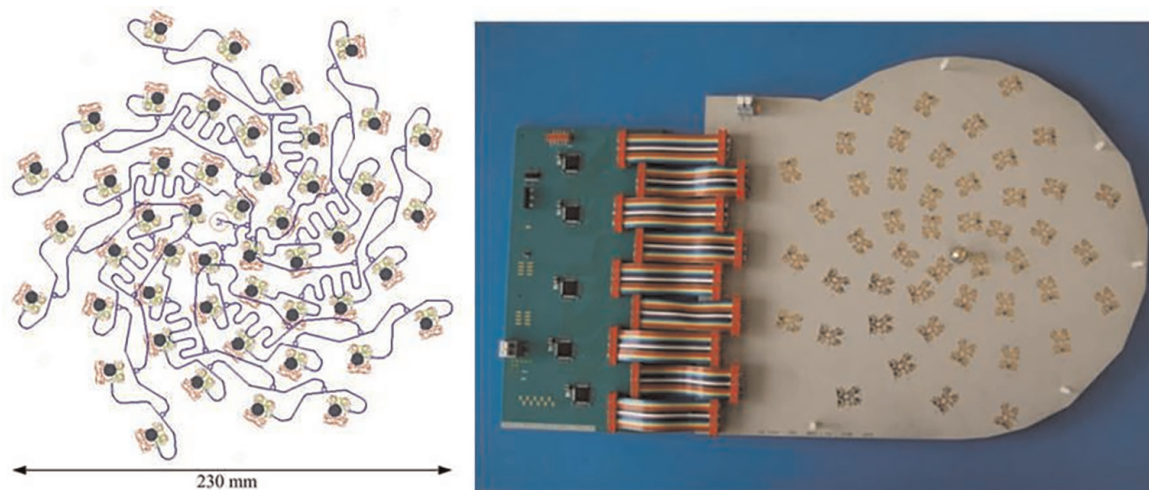


Figure 12. Aperiodic sparse array phased array antenna experimental system for satellite communication on the ground.

In 2014, Maria Carolina Viganó of ViaSat Antenna Systems in Switzerland and others completed the research and development of the ground-side aperiodic sparse array phased array antenna experimental system for satellite communication with the special support of ESA [45]. The system works in the Ka-band and adopts 1-bit quantization phase control, and its design is based on a novel sunflower arrangement, as shown in **Figure 12** [56]. The left picture shows the array topology and the distribution of the feeding network, and the right picture shows the finished experimental sample. The test results show that the antenna has reached the basic design index and has good development potential.

The application of aperiodic array phased array antenna in spaceborne SAR systems began in the 21st century. ESA and the National Aeronautics and Space Administration (NASA) have funded a number of research institutions to carry out research on Spaceborne SAR sparse array or aperiodic array phased array antenna, and have made some research progress in array synthesis technology, aperiodic array imaging technology, and hardware implementation scheme.

In terms of aperiodic array synthesis technology for Spaceborne SAR requirements, ESA and Cristian Iuon and Stefano Selleri of the University of Florence in Italy published an important research paper on the application of aperiodic array phased array antenna to spaceborne SAR in 2012 [36]. This paper presents a practical method for Spaceborne SAR aperiodic array synthesis, which is divided into three steps: firstly, according to the task requirements of spaceborne SAR, the synthesis of a single excitation amplitude distribution pattern based on the traditional periodic array is completed; secondly, according to the results of the amplitude distribution of periodic array, the aperiodic sparse array is obtained by amplitude density taper transformation; finally, the element position and excitation phase of the sparse array are optimized to make the final design results meet the beam performance requirements. As shown in **Figure 13**, the upper part of the figure shows the three-step design process and the schematic diagram of array element distribution obtained in each step. Starting from the initial 64-element periodic array, a 48-element linear array with constant amplitude excitation is obtained after the second step of thinning, and then the final aperiodic array unit position and excitation phase distribution are obtained through the third step of array element position optimization. The lower part of **Figure 13** shows the patterns generated by the designed aperiodic array to meet the beam requirements of two different spaceborne SAR. Both patterns are generated by

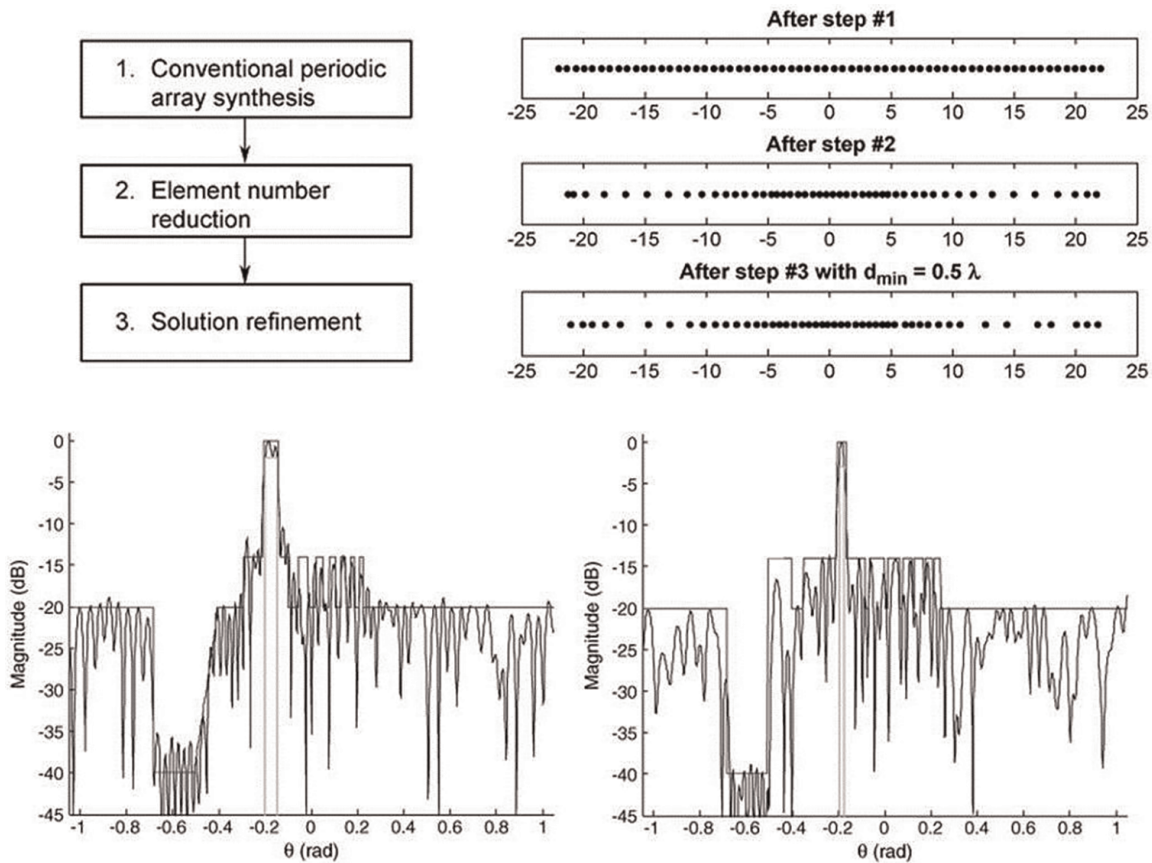


Figure 13.
 Results of spaceborne SAR aperiodic array antenna.

the same aperiodic array with equal amplitude excitation, and only the excitation phase distribution is different.

Although it can significantly improve the system performance in theory, the engineering realization of aperiodic array antenna is very difficult, and the development of related technologies is not mature. Therefore, from the perspective of ensuring system reliability and avoiding technical risks, the conditions for applying aperiodic array phased array antennas in spaceborne SAR systems with high R&D costs and a small number are not yet mature.

4. Technical features and development of spaceborne SAR parabolic phased array antenna

TanDEM-L is a spaceborne distributed SAR satellite plan proposed by Deutsches Zentrum für Luft-und Raumfahrt (DLR). The plan consists of two L-band spaceborne SAR systems. The schematic diagram of the concept is shown in **Figure 14**. The program was developed to monitor dynamic changes on the Earth's surface such as forest biomass, millimeter-scale surface deformation, polar ice, and soil moisture. In the TanDEM-L plan, the inversion of vegetation parameters, stereo imaging, and surface deformation monitoring technology are realized through polarization interference, multi-baseline, and heavy orbit technology, which are helpful for a better understanding of the earth system, risk analysis, disaster management, and environmental monitoring are of great significance (**Figure 14**) [57].

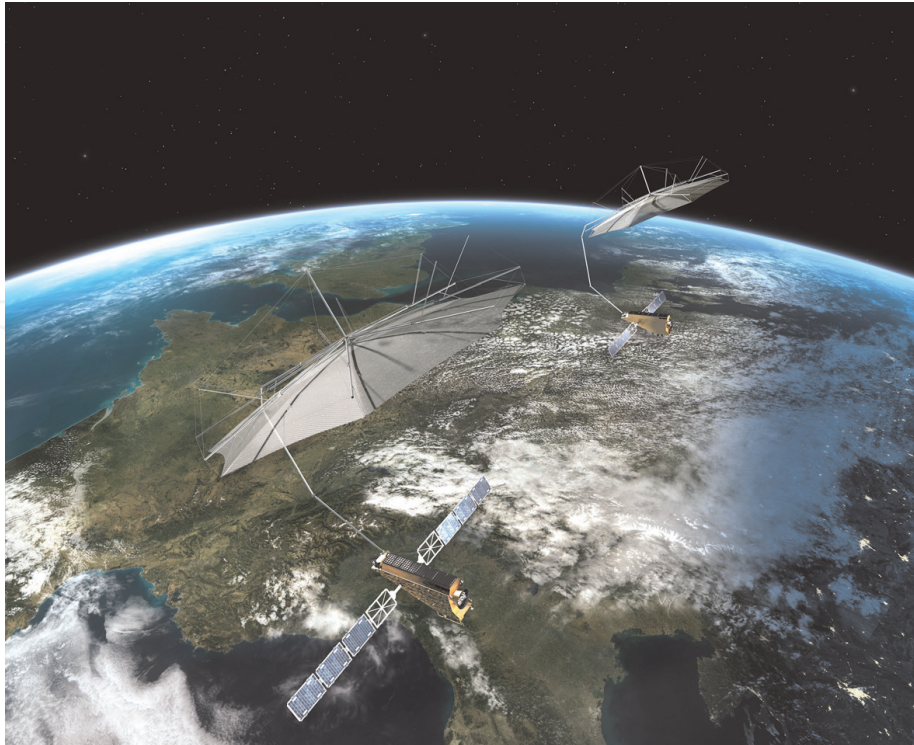


Figure 14.
Preview of TanDEM-L Plan.

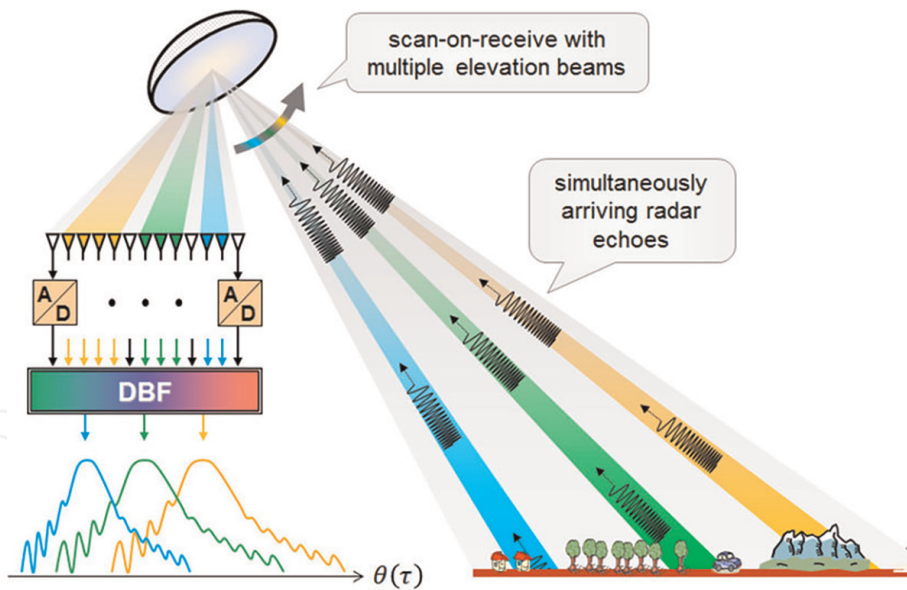


Figure 15.
Example of Elevation multibeam reflector SAR system.

Technologies such as parabolic reflector antenna, DBF technology (as shown in **Figure 15**), and variable PRF technology are used in the TanDEM-L satellite program. Through the combination of these technologies, TanDEM-L plans to achieve 3 m resolution, 350 km wide Earth observation, and the ability to realize a dynamic observation of the world in 6 days. Among these technologies, the combination of reflector antenna and DBF technology is used to achieve high gain acceptance through distance scanning and improve the system signal-to-noise ratio; variable PRF technology changes the position of the blind spot to achieve continuous imaging of the scene [58].

A major feature of the TanDEM-L program is the use of a combination of a deployable reflector antenna and a two-dimensional digital feed array (**Figure 16**). The left image is a technical solution proposed by DLR researchers to combine a reflector antenna and a two-dimensional digital feed array. In this scheme, the diameter of the reflector antenna is 15 m, and the feed source is a digital array of 36 (elevation) \times 3 (azimuth) and aligned horizontally. The scheme achieves a wide range and high gain in the distance direction by using the scanning processing concept of “Scan-On-Receive”. Each of the pitch array elements consists of dual-polarized microstrip patches, and the signal from each polarization port is routed through the TR assembly and digitized in the corresponding DBF unit [58].

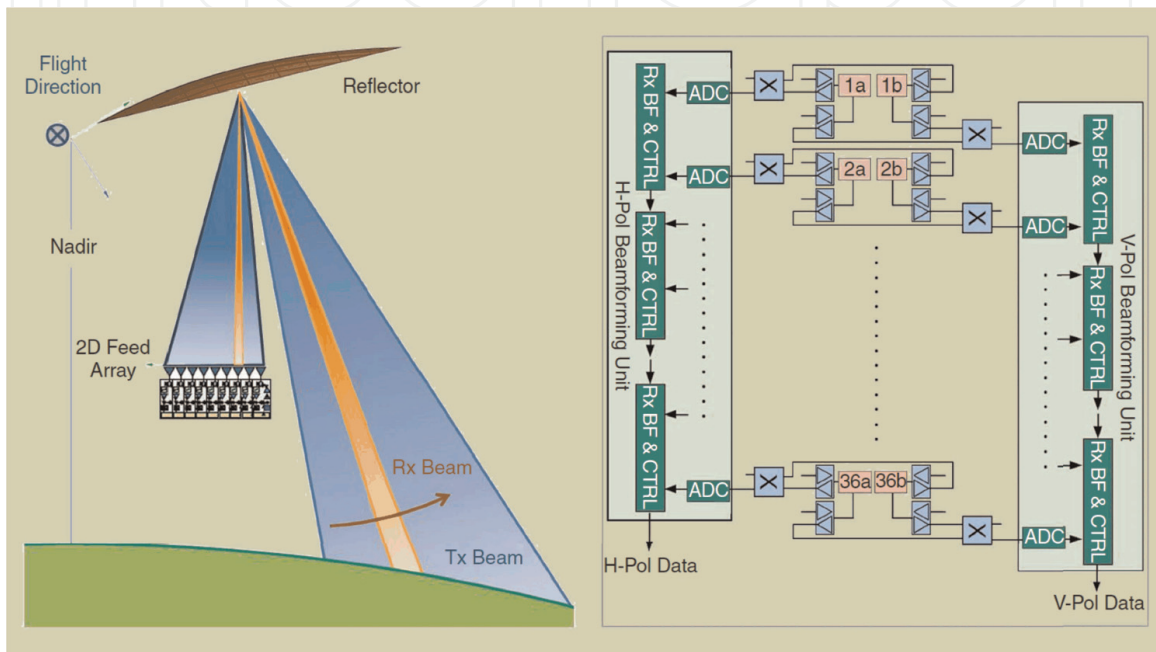


Figure 16.
 Reflector and feed array of TanDEM-L.

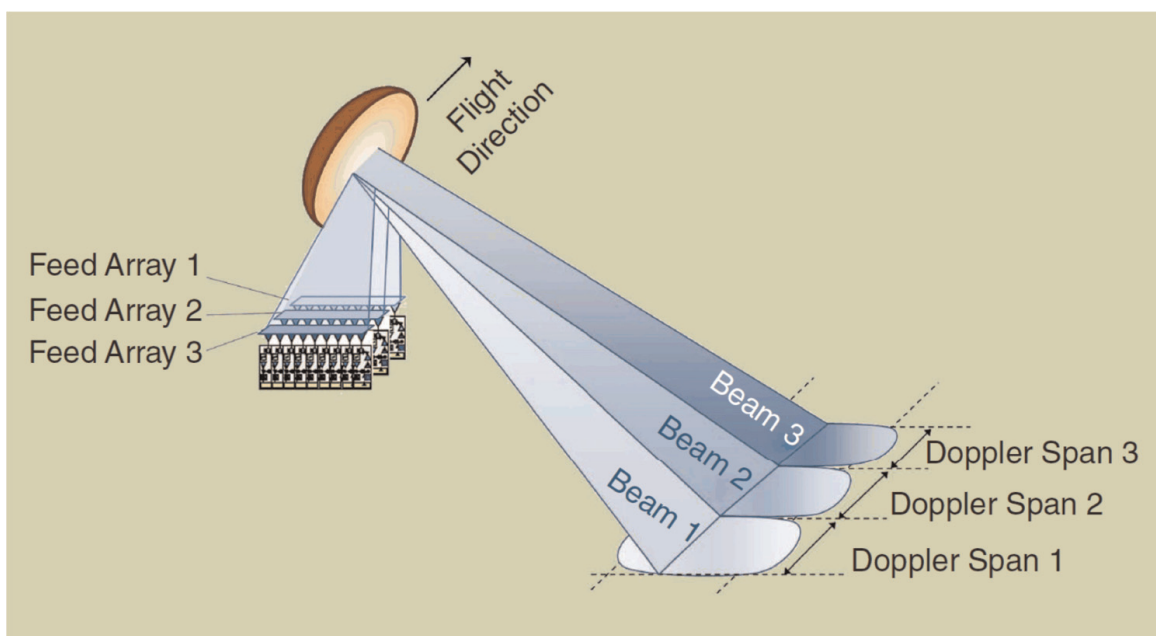


Figure 17.
 Three azimuthal feed arrays antenna of TanDEM-L.

This scheme achieves high resolution in azimuth by adding the feed array and azimuth beamforming technology in **Figure 16** along the azimuth. As shown in **Figure 17**, each feed array corresponds to an azimuth channel transformed to the ground, and the overall azimuth spectrum is recovered by beamforming technology.

5. Technical features and development of spaceborne SAR plane reflector metasurface phased array antenna

The Capella X-SAR satellite constellation plan is a constellation plan proposed by Capella Space, which consists of 36 spaceborne SAR systems. 36 SAR satellites form 12 orbital planes, each operating in a 500 km polar orbit with an orbital period of 90 min, providing average imaging revisit time of less than 1 h. Capella’s 01 star Denali was launched as a test star in December 2018. The star uses an “origami-type” planar reflector metasurface antenna (as shown in **Figure 18** left). The launch time of subsequent stars is shown in **Table 2**. It is a meshed reflector antenna with a peripheral frame structure (as shown in **Figure 18** right) [59].

Capella’s 01 satellite, Denali, was launched as a test satellite, which is the size of a backpack and has a mass of about 40 kg. When designing Denali’s SAR payload, the researchers combined an origami-shaped antenna with efficient electronics. Among



Figure 18. Plane reflector metasurface array antenna of Capella X-SAR plan.

Satellite	Date
Capella 2 (Sequoia)	2020.08.31
Capella 3 (Whitney 1)	2021.01.24
Capella 4 (Whitney 2)	2021.01.24
Capella 5 (Whitney 3)	2021.06.30
Capella 6 (Whitney 4)	2021.05.15
Capella 7 (Whitney 5)	2022.01.13
Capella 8 (Whitney 6)	2022.01.13
Capella 9	2022(plan)

Table 2. Capella X-SAR plan.

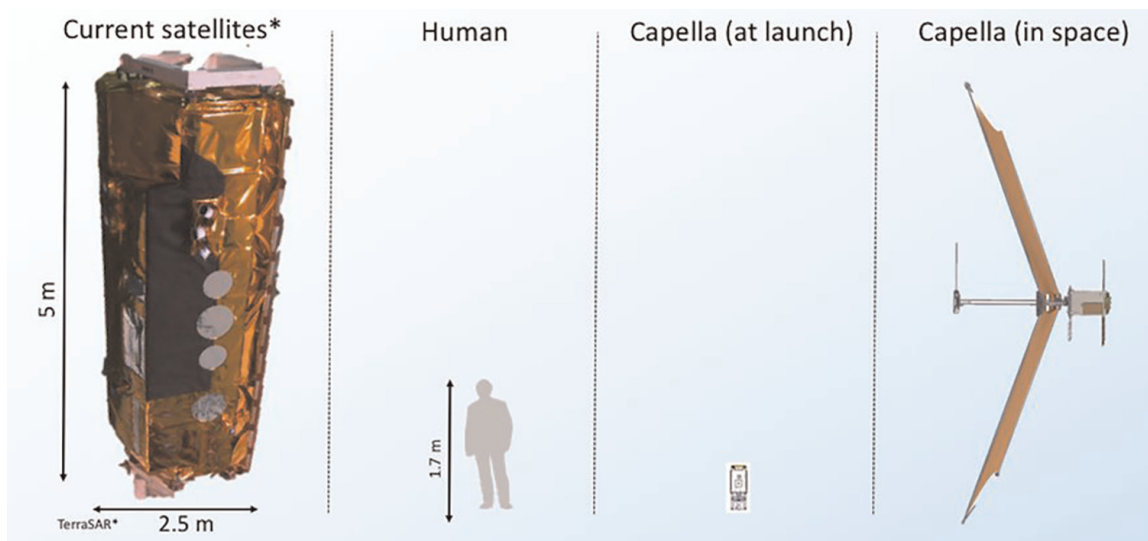


Figure 19.
Example of array antenna of Capella satellite.

them, the antenna is made of flexible material, and the area is about 8 m^2 after deployment. Columns 3 and 4 in **Figure 19** are the dimensions of the Denali satellite before and after deployment [60].

6. Conclusions

A large-scale array antenna is one of the core components of high-performance spaceborne SAR, which determines the performance of spaceborne SAR to a great extent. The traditional spaceborne SAR phased array antenna adopts the periodic array implementation scheme, which has the advantages of strong beam control ability, sufficient failure redundancy backup, mature design method, and so on. It has been widely used in the existing spaceborne SAR system. However, the phased array antenna based on the periodic array scheme has the disadvantages of large size, heavy weight, high manufacturing cost, and low energy utilization, which restricts the further improvement of the performance of the spaceborne SAR system and the research and development of the next generation of high-performance spaceborne SAR system. Using aperiodic array antenna, parabolic array antenna and hypersurface array antenna have the possibility to overcome the above shortcomings. Based on the technical characteristics and development trend of spaceborne SAR array antenna, this article reviews the theoretical analysis, simulation results, and experimental verification.

Acknowledgements

The author would like to thank Y. Wen and J. Wang for their tremendous help and technical discussions.

IntechOpen


IntechOpen

Author details

Hua Li, Zhenning Li, Kaiyu Liu, Mingshan Ren and Yunkai Deng
Department of Space Microwave Remote Sensing System, Aerospace Information
Research Institute, Chinese Academy of Sciences, Beijing, China

*Address all correspondence to: fiskli@foxmail.com

IntechOpen

© 2022 The Author(s). Licensee IntechOpen. This chapter is distributed under the terms of the Creative Commons Attribution License (<http://creativecommons.org/licenses/by/3.0>), which permits unrestricted use, distribution, and reproduction in any medium, provided the original work is properly cited. 

References

- [1] Elachi C, Bicknell T, Jordan RL, Chilin W. Spaceborne synthetic-aperture imaging radars: Applications, techniques, and technology. *Proceedings of the IEEE*. 1982;**70**:1174-1209. DOI: 10.1109/PROC.1982.12448
- [2] L band Mission – Seasat 1 [EB/OL]. 2014. Available from: <https://directory.eoportal.org/web/eoportal/satellite-missions/s/seasat>
- [3] S band NovaSAR-S [EB/OL]. 2015. Available from: <https://directory.eoportal.org/web/eoportal/satellite-missions/n/novasar-s>
- [4] C band Copernicus: Sentinel-1 [EB/OL]. 2014. Available from: <https://directory.eoportal.org/web/eoportal/satellite-missions/c-missions/copernicus-sentinel-1>
- [5] X band TecSAR [EB/OL]. 2008. Available from: <https://directory.eoportal.org/web/eoportal/satellite-missions/t/tecsar>
- [6] C band RADARSAT-2 [EB/OL]. 2007. Available from: <https://directory.eoportal.org/web/eoportal/satellite-missions/r/radarsat-2>
- [7] COSMO-SkyMed, eoPortal Directory [EB/OL]. 2007. Available from: <https://directory.eoportal.org/web/eoportal/satellite-missions/c-missions/cosmo-skymed>
- [8] X band Terra-SAR [EB/OL]. 2007. Available from: <https://directory.eoportal.org/web/eoportal/satellite-missions/t/terrasar-x>
- [9] Berger M, Moreno J, Johannessen JA, Levelt PF, Hanssen RF. ESA's sentinel missions in support of Earth system science. *Remote Sensing of Environment*. 2012;**120**:84-90. DOI: 10.1016/j.rse.2011.07.023
- [10] SIR-A [EB/OL]. 1981. Available from: <https://directory.eoportal.org/web/eoportal/satellite-missions/s/sir-a>
- [11] Rosenqvist A, Shimada M, Watanabe M. L band ALOS PALSAR: Technical outline and mission concepts. In: 4th International Symposium on Retrieval of Bio- and Geophysical Parameters from SAR Data for Land Applications; Innsbruck, Austria, 16-19 November 2004. pp. 1-7
- [12] Li FK, Johnson W. Ambiguities in spaceborne synthetic aperture radar systems. *IEEE Transactions on Aerospace and Electronic Systems*. 1983;**19**:389-397. DOI: 10.1109/TAES.1983.309319
- [13] X band COSMO-SkyMed System Description and User Guide [EB/OL]. 2007. Available from: http://www.egeos.it/products/pdf/csk-user_guide.pdf
- [14] Torre A, P C. X band COSMO-SkyMed: The advanced SAR instrument. In: 5th International Conference on Recent Advances in Space Technologies (RAST '11); 9–11 June 2011. Istanbul, New York: IEEE; 2011. pp. 865-868
- [15] Ka M, Kononov AA. Effect of look angle on the accuracy performance of fixed-baseline interferometric SAR. *IEEE Geoscience and Remote Sensing Letters*. 2007;**4**:65-69. DOI: 10.1109/LGRS.2006.885858
- [16] Onwujekwe O, Uguru N, Russo G, Etiaba E, Mbachu C, Mirzoev T, et al. Role and use of evidence in policymaking: an analysis of case studies from the health sector in Nigeria. *Health Research Policy and Systems*. 2015;**13**:46. DOI: 10.1186/s12961-015-0049-0

- [17] Capece P, Borgarelli L, Di Lazzaro M, Di Marcantonio U, Torre A. Cosmo Skymed active phased array SAR instrument. In: Radar Conference (RADAR '08); 26–30 May 2008. Rome, New York: IEEE; 2008. pp. 1-4
- [18] Grafmuller B, Herschlein A, Fischer C. The TerraSAR-X antenna system. In: Radar Conference (RADAR '05); 9–12 May 2005. Arlington VA. New York: IEEE; 2005. pp. 222-225
- [19] Ostergaard A, Snoeij P, Traver IN, Ludwig M, Rostan F, Croci R. C-band SAR for the GMES Sentinel-1 mission. In: 8th European Radar Conference (EURAD'11); 12–14 October 2011; Manchester. New York: IEEE; 2011. pp. 234-240
- [20] Schoenfeld U, Braudach H. Electrical architecture of the SENTINEL-1 SAR antenna subsystem. In: 7th European Conference on Synthetic Aperture Radar (EUSAR '08); 2–5 June 2008; Friedrichshafen. New York: IEEE; 2008. pp. 1-4
- [21] Zhang HT, Wang W, Zhang ZH. Ridged waveguide slot antenna array with low cross-polarization. In: International Conference on Microwave and Millimeter Wave Technology (ICMMT '12); 5–8 May 2012; Shenzhen. New York: IEEE. pp. 1-3
- [22] Mehdipour A, Sebak AR, Truemen CW. Conductive carbon fiber composite materials for antenna and microwave applications. In: 29th National Radio Science Conference (NRSC '12); 10–12 April 2012; Cairo. New York: IEEE. pp. 1-8
- [23] Wagner R, Braun HM. A slotted waveguide array antenna from carbon fibre reinforced plastics for the European space SAR. *Acta Astronautica*. 1980;8: 273-282. DOI: 10.1016/0094-5765(81)90036-9
- [24] Zahn R, Kirscht M, Weidmann K. Modular Radar Core for airborne and space applications. *IEEE International Geoscience and Remote Sensing Symposium*. 2010;2010:677-680. DOI: 10.1109/IGARSS.2010.5651829
- [25] Moussessian A, Delcastillo L, Bach V, Grando M, Quijano U, Smith P, et al. Large aperture, scanning, L-Band SAR. In: NASA Earth Science Technology Conference, June 21, 2011, Pasadena, California. pp. 1-4. DOI: 10.1049/joe.2019.0602
- [26] Leipold M, Runge H, Sickinger C. Large Sar Membrane Antennas With Lightweight Deployable Booms. In: 28th ESA Antenna Workshop on Space Antenna Systems and Technologies. 2005. pp. 1-8
- [27] Wang HJ, Fan B, Yi M, Guan FL, Guang L, Xue C, et al. Inflatable Antenna for Space-Borne Microwave Remote Sensing. *IEEE Antennas and Propagation Magazine*. 2012;54:58-70. DOI: 10.1109/MAP.2012.6348118
- [28] Di Lorenzo P, Barbarossa S, Borgarelli L. Optimal Beamforming for Range-Doppler Ambiguity Minimization in Squinted SAR. *IEEE Transactions on Aerospace and Electronic Systems*. 2013;49:277-293. DOI: 10.1109/TAES.2013.6404103
- [29] Zeng XN, He F, Zhang YS, Dong Z. Analysis and compensation of spaceborne SAR antenna array deformation. *Journal of National University of Defense Technology*. 2012;34:158-163. DOI: 10.3969/j.issn.1001-2486.2012.03.031
- [30] Wolff I. From antennas to microwave systems-LTCC as an

integration technology for space applications. In: 3rd European Conference on Antennas and Propagation (EuCAP '09); 23–27 March 2009; Berlin. New York: IEEE; 2009. pp. 3-8

[31] Florian C, Traverso PA, Feudale M, Filicori F. A C-band GaAs-pHEMT MMIC low phase noise VCO for space applications using a new cyclostationary nonlinear noise model. In: IEEE MTT-S International Microwave Symposium (IMS '10); 23–28 May 2010; Anaheim CA. New York: IEEE; 2010. pp. 284-287

[32] Cao MY, Zhang K, Chen YH, Zhang JC. High-efficiency S-band harmonic tuning GaN amplifier. *Chinese Physics B*. 2014;23:37305. DOI: 10.1088/1674-1056/23/3/037305

[33] Attema EPW. The Active Microwave Instrument On-Board the ERS-1 Satellite. *Proceedings of the IEEE*. 2002; 79:761-799. DOI: 10.1109/5.90158

[34] Buckreuss S, Steinbrecher U, Schattler B. The TerraSAR-X Mission Status. In: Asian and Pacific Conference on Synthetic Aperture Radar (APSAR '15); 1–4 September 2015; Singapore. New York: IEEE; 2015. pp. 357-361

[35] Valerio G, Barbara B, Pasquale S, Perrera A, Pepe P, Inversi P, et al. CSK mission status and experimentation results. In: 11th European Conference on SAR (EUSAR '16); 6–9 June 2016; Hamburg. New York: IEEE; 2016. pp. 1-3

[36] Luison C, Landini A, Angeletti P, Toso G, Valle P, Capece P, et al. Aperiodic Arrays for Spaceborne SAR Applications. *IEEE Transactions on Antennas and Propagation*. 2012;60: 2285-2294. DOI: 10.1109/TAP.2012.2189714

[37] Catalani A, Russo L, Bucci O M, T. Isernia: “Sparse Arrays for Satellite Communications: From Optimal Design to Realization”. *Proceedings of the 32nd ESA Antenna Workshop on Antennas for Space Applications*. 2010. p. 5-8. DOI: 10.1109/APS.2012.6348916

[38] Angeletti P, Toso G. Aperiodic arrays for space applications: A combined amplitude/density synthesis approach. In: 3rd European Conference on Antennas and Propagation (EuCAP '09); 23–27 March 2009; Berlin. New York: IEEE; 2009. pp. 2026-2030

[39] Toso G, Angeletti P, Mangenot C. A comparison of density and amplitude tapering for transmit active arrays. In: 3rd European Conference on Antennas and Propagation (EuCAP '09); 23-27 March 2009; Berlin. New York: IEEE; 2009. pp. 840-843

[40] Ishimaru A. Theory of unequally-spaced arrays. *IRE Transactions on Antennas and Propagation*. 1962;10: 691-702. DOI: 10.1109/TAP.1962.1137952

[41] Pierro V, Galdi V, Castaldi G, Pinto IM, Felsen LB. Radiation properties of planar antenna arrays based on certain categories of aperiodic tilings. *IEEE Transactions on Antennas and Propagation*. 2005;53:635-644. DOI: 10.1109/TAP.2004.841287

[42] Lu J, Guo Y. Novel aperiodic phased array with reduced number of active chains for space-borne SAR. In: 5th Asia-Pacific Conference on Synthetic Aperture Radar (APSAR '15); 1-4 September 2015; Singapore. New York: IEEE. pp. 20-23

[43] Lu J, Guo Y, Yang H. Sparse phased array antenna for space-borne SAR. In: *International Symposium on Antennas and Propagation (ISAP '15)*; 19–24 July

2015; Vancouver. New York: IEEE; 2015. pp. 2461-2462

[44] Lu J, Guo Y. Compact Planar Sparse Array Antenna with Optimum Element Dimensions for SATCOM Ground Terminals. *International Journal of Antennas and Propagation*. 2015;806981. DOI: 10.1155/2015/806981

[45] Viganó MC, Llorens Del Rio D, Bongard F, Bongard F, Vaccaro S. Sparse Array Antenna for Ku-Band Mobile Terminals Using 1 Bit Phase Controls. *IEEE Transactions on Antennas and Propagation*. 2014;62:1723-1730. DOI: 10.1109/TAP.2014.2301439

[46] Skobelev SP. One more look at the reduction of the number of controlled elements in limited-scan phased array antennas. In: 8th European Conference on Antennas and Propagation (EuCAP '14); 6-11 April 2014; The Hague. New York: IEEE; 2014. pp. 3625-3628

[47] Angeletti P, Toso G. Array antennas with jointly optimized elements positions and dimensions part I: Linear arrays. *IEEE Transactions on Antennas and Propagation*. 2014;62:1619-1626. DOI: 10.1109/TAP.2013.2281602

[48] Angeletti P, Toso G, Ruggerini G. Array Antennas with Jointly Optimized Elements Positions and Dimensions Part II: Planar Circular Arrays. *IEEE Transactions on Antennas and Propagation*. 2014;62:1627-1639. DOI: 10.1109/TAP.2013.2281519

[49] Bucci OM, Isernia T, Perna S, Pinchera D. Isophoric sparse arrays ensuring global coverage in satellite communications. *IEEE Transactions on Antennas and Propagation*. 2014;62:1607-1618. DOI: 10.1109/TAP.2013.2287901

[50] Johansson S. Design Study into Sparse Array Antenna Demonstrators for Future Satellite Systems[D]. Gothenburg: Ghalmers University of Technology; 2014

[51] Catalani A, Russo L, Isernia T, Toso G, Angeletti P. Ka-Band active sparse arrays for SATCOM applications. In: *International Symposium on Antennas and Propagation (ISAP '12)*; 8-14 July 2012; Chicago. New York: IEEE; 2012. pp. 1-2

[52] Toso G, Mangenot C, Roederer AG. Sparse and thinned arrays for multiple beam satellite applications. In: *2nd European Conference on Antennas and Propagation (EuCAP '07)*; 11-16 November 2007; Edinburgh. New York: IEEE; 2008. pp. 1-4

[53] Lu J, Yang H, Wen G, Li D. An aperiodic phased array antenna for space-borne Synthetic Aperture Radar. In: *Loughborough Antennas & Propagation Conference (LAPC '16)*; 14-15 November 2016; Loughborough. New York: IEEE; 2017. pp. 1-5

[54] Caratelli D, Viganó MC. Analytical synthesis technique for linear uniform-amplitude sparse arrays. *Radio Science*. 2011;46:1-6. DOI: 10.1029/2010RS004522

[55] Bucci OM, D'Urso M, Isernia T, Angeletti P, Toso G. Deterministic synthesis of uniform amplitude sparse arrays via new density taper techniques. *IEEE Transactions on Antennas and Propagation*. 2010;58:1949-1958. DOI: 10.1109/TAP.2010.2046831

[56] Viganó MC, Toso G, Caille G, Cyril M, Lager I. Sunflower array antenna with adjustable density taper. *International Journal of Antennas and Propagation*. 2009;2009:1-10. DOI: 10.1155/2009/624035

[57] Younis M et al. Tandem-L instrument design and SAR performance overview. IEEE Geoscience and Remote Sensing Symposium. 2014;2014:88-91. DOI: 10.1109/IGARSS.2014.6946362

[58] Klenk P, Reimann J, Schwerdt M. Performance aspects of large-deployable reflector antennas based on surface deformations simulated for tandem-L. In: 2019 13th European Conference on Antennas and Propagation (EuCAP). 2019. pp. 1-5

[59] Stringham C et al. The Capella X-band SAR constellation for rapid imaging. In: IGARSS 2019 – 2019 IEEE International Geoscience and Remote Sensing Symposium. 2019. pp. 9248-9251. DOI: 10.1109/IGARSS.2019.8900410

[60] Castelletti D, Farquharson G, Stringham C, Duersch M and Eddy D. "Capella Space First Operational SAR Satellite". 2021 IEEE International Geoscience and Remote Sensing Symposium IGARSS. 2021. p. 1483-1486. DOI:10.1109/IGARSS47720.2021.9554100